

Optimal parameter combinations of entanglement in the general Heisenberg model

Da-Chuang Li(李大创), Wei-Wei Pan(潘维韦), Xing-Dong Zhao(赵兴东), and Xiao-Lan Zong(宗晓岚)
Citation: Chin. Phys. B, 2025, 34 (**10**): 100308. DOI: 10.1088/1674-1056/adec5c
http://cpb.iphy.ac.cn; http://iopscience.iop.org/cpb

What follows is a list of articles you may be interested in

Quantum-enhanced time-of-arrival measuring method based on partially entangled state

Peng-Xian Li(李芃鲜), Lu-Ping Xu(许录平), Gui-Ting Hu(胡桂廷), and Wen-Long Gao(高文珑)
Chin. Phys. B, 2025, 34 (**7**): 070303. DOI: 10.1088/1674-1056/adc7ee

Measurement-based entanglement purification for hybrid entangled state

Cheng-Chen Luo(罗程晨), Shi-Pu Gu(顾世浦), Xing-Fu Wang(王兴福), Lan Zhou(周澜), and Yu-Bo Sheng(盛宇波)
Chin. Phys. B, 2025, 34 (**3**): 030307. DOI: 10.1088/1674-1056/adb267

A pure quantum secret sharing scheme based on GHZ basis measurement and quantum entanglement exchange

Bai Liu(刘白), Jun Zhang(张俊), Shupin Qiu(邱书品), and Mingwu Zhang(张明武)
Chin. Phys. B, 2025, 34 (**3**): 030304. DOI: 10.1088/1674-1056/ada548

Entanglement and energy transportation in central-spin quantum battery

Fan Liu(刘帆), Hui-Yu Yang(杨慧宇), Shuai-Li Wang(王帅立), Jun-Zhong Wang(王俊钟), Kun Zhang(张堃), and Xiao-Hui Wang(王晓辉)
Chin. Phys. B, 2025, 34 (**2**): 020306. DOI: 10.1088/1674-1056/ad9a9d

Enhancing entanglement and steering in a hybrid atom-optomechanical system via Duffing nonlinearity

Ling-Hui Dong(董凌晖), Xiao-Jie Wu(武晓捷), Cheng-Hua Bai(白成华), and Shao-Xiong Wu(武少雄)
Chin. Phys. B, 2025, 34 (**2**): 020304. DOI: 10.1088/1674-1056/ad9ba2

RAPID COMMUNICATION

Optimal parameter combinations of entanglement in the general Heisenberg model

Da-Chuang Li(李大创)[1,2], Wei-Wei Pan(潘维韦)[1], Xing-Dong Zhao(赵兴东)[3], and Xiao-Lan Zong(宗晓岚)[1,†]

[1] *School of Physics and Materials Engineering, Hefei Normal University, Hefei* 230601, *China*

[2] *Key Laboratory of Quantum Information and Department of Modern Physics, University of Science and Technology of China, Hefei* 230026, *China*

[3] *School of Physics, Henan Normal University, Xinxiang* 453007, *China*

(Received 22 April 2025; revised manuscript received 16 June 2025; accepted manuscript online 7 July 2025)

Thermal entanglement, as influenced by interaction parameters, is investigated within the general Heisenberg XYZ model. We calculate the relationship between entanglement and the system interaction parameters, including spin–spin interaction parameters (SSIPs) and spin–orbit interaction parameters (SOIPs). By considering various parameter orientations, we identify four optimal combinations of the SSIPs and find that the optimal vector of the spin–orbit interaction aligns with the coordinate axis corresponding to the maximal SSIP component. Furthermore, we obtain three effective optimal combinations of the SOIPs corresponding to the optimal SSIPs, which can maximize the system entanglement when the parameters are tuned accordingly. To demonstrate the feasibility of our results under realistic experimental conditions, we propose an optical lattice scheme with tunable parameters.

Keywords: entanglement, Heisenberg model, Dzyaloshinskii–Moriya interaction

PACS: 03.65.Ud, 03.67.Bg, 75.10.Jm

DOI: 10.1088/1674-1056/adec5c **CSTR:** 32038.14.CPB.adec5c

1. Introduction

Entanglement has been extensively studied in recent years due to its fascinating nonclassical nature in quantum mechanics and its key role in quantum information processing.[1–7] Recently, the Heisenberg model has been extensively studied. As a simple model, it is considered an ideal candidate for the generation and manipulation of entangled states. This model has been used to simulate various solid-state physical systems, such as nuclear spins,[8,9] optical lattices,[10–12] quantum dots,[13–18] and superconductors.[19–22] To quantitatively and qualitatively characterize entanglement in solid-state systems and exploit it for quantum information applications, thermal entanglement properties in the Heisenberg model have been extensively investigated.[23–29] Building on this work, we further explored the impact of parameter directions on system entanglement.[30–33] In particular, in Ref. [31], we found that higher entanglement can be achieved by tuning the direction of the external magnetic field.

In this paper, to thoroughly explore the influence of parameters on entanglement, we conduct a detailed study of the correlation between parameter directions and system entanglement. We identify the optimal combinations of various parameters, namely, four optimal combinations of spin–spin interaction parameters (SSIPs) and three optimal combinations of spin–orbit interaction parameters (SOIPs) corresponding to the optimal SSIPs. Furthermore, we establish the criteria for determining optimal SOIP combinations: the optimal direction of the spin–orbit interaction vector is parallel to the coordinate axis along which the SSIP has the maximal component. Therefore, for given parameter values, the maximal system entanglement can be obtained by adjusting the parameters to their optimal combinations. Moreover, we propose a physical scheme for tuning system parameters in an optical lattice.

This paper is organized as follows. In Section 2, we investigate the optimal combinations of SSIPs and identify four optimal cases. In Section 3, we study the optimal combinations of SOIPs and obtain three effective cases. In Section 4, we construct the general Heisenberg model in an optical lattice and discuss the experimental feasibility of parameter adjustment. Finally, in Section 5, we present a discussion and conclusion.

2. Optimal combination of SSIPs

The Hamiltonian H for the general two-qubit Heisenberg XYZ model is

$$H = J_x\sigma_1^x\sigma_2^x + J_y\sigma_1^y\sigma_2^y + J_z\sigma_1^z\sigma_2^z, \tag{1}$$

where σ^i $(i = x,y,z)$ are Pauli matrices, and J_i $(i = x,y,z)$ denotes the SSIP along the i-axis. All parameters in this paper are dimensionless. For convenience in illustrating our ideas, the set of SSIPs can be regarded as a vector $\boldsymbol{J}$ with $|\boldsymbol{J}| = 1$, where J_i $(i = x,y,z)$ is the i-axis component of $\boldsymbol{J}$.

†Corresponding author. E-mail: xlzong725@foxmail.com

© 2025 Chinese Physical Society and IOP Publishing Ltd. All rights, including for text and data mining, AI training, and similar technologies, are reserved.

Thus, according to Fig. 1, the components J_i can be expressed in the spherical coordinate system as $J_x = \sin\theta_0\cos\phi_0$, $J_y = \sin\theta_0\sin\phi_0$, and $J_z = \cos\theta_0$.

In the standard basis $\{|00\rangle, |01\rangle, |10\rangle, |11\rangle\}$, a straightforward calculation yields the eigenstates of H: $|\Psi_{1,2}\rangle = \frac{1}{\sqrt{2}}(|00\rangle \pm |11\rangle)$ and $|\Psi_{3,4}\rangle = \frac{1}{\sqrt{2}}(|01\rangle \pm |10\rangle)$, with the corresponding eigenvalues given by $E_{1,2} = \cos\theta_0 \pm \sin\theta_0\cos\phi_0 \mp \sin\theta_0\sin\phi_0$ and $E_{3,4} = -\cos\theta_0 \pm \sin\theta_0\cos\phi_0 \pm \sin\theta_0\sin\phi_0$. In this case, the thermal equilibrium state of the system can be written as

$$\rho(T) = \frac{1}{2Z}\begin{pmatrix} e^{-\frac{E_1}{T}} + e^{-\frac{E_2}{T}} & 0 & 0 & e^{-\frac{E_1}{T}} - e^{-\frac{E_2}{T}} \\ 0 & e^{-\frac{E_3}{T}} + e^{-\frac{E_4}{T}} & e^{-\frac{E_3}{T}} - e^{-\frac{E_4}{T}} & 0 \\ 0 & e^{-\frac{E_3}{T}} - e^{-\frac{E_4}{T}} & e^{-\frac{E_3}{T}} + e^{-\frac{E_4}{T}} & 0 \\ e^{-\frac{E_1}{T}} - e^{-\frac{E_2}{T}} & 0 & 0 & e^{-\frac{E_1}{T}} + e^{-\frac{E_2}{T}} \end{pmatrix}, \tag{2}$$

where

$$Z = 2e^{-\frac{\cos\theta_0}{T}}\cosh\left(\frac{\sin\theta_0(\cos\phi_0 - \sin\phi_0)}{T}\right) + 2e^{\frac{\cos\theta_0}{T}}\cosh\left(\frac{\sin\theta_0(\cos\phi_0 + \sin\phi_0)}{T}\right),$$

which represents the partition function of the system.

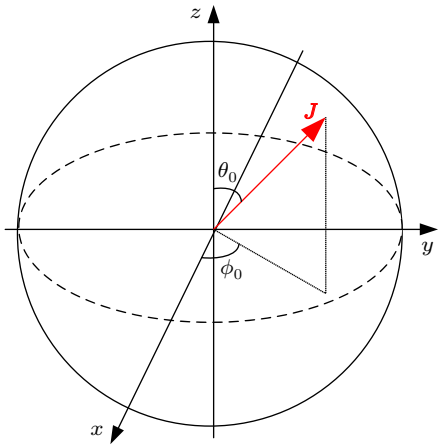


Fig. 1. Spin–spin interaction vector $\boldsymbol{J}$ represented in the spherical coordinate system.

In the following, we employ the negativity introduced by Vidal and Werner[34] as the entanglement measure. The negativity N of a state ρ is defined as $N(\rho) = \frac{\|\rho^{T_1}\|-1}{2} = \frac{\sum_i|\lambda_i|-1}{2}$, where ρ^{T_1} is the partial transpose of the density matrix ρ with respect to the first subsystem, and λ_i are the eigenvalues of ρ^{T_1} given by $\lambda_{1,2} = \frac{1}{2Z}(e^{-\frac{E_1}{T}} + e^{-\frac{E_2}{T}} \pm e^{-\frac{E_3}{T}} \mp e^{-\frac{E_4}{T}})$ and $\lambda_{3,4} = \frac{1}{2Z}(\pm e^{-\frac{E_1}{T}} \mp e^{-\frac{E_2}{T}} + e^{-\frac{E_3}{T}} + e^{-\frac{E_4}{T}})$. Based on the above calculation, we plotted Fig. 2 to analyze the optimal combination of SSIPs. Theoretically, the negativity varies periodically with the variables θ_0 and ϕ_0, implying infinitely many optimal combinations. However, due to the restricted ranges of these variables, i.e., $\theta_0 \in [0,\pi]$ and $\phi_0 \in [0,2\pi]$, only four optimal combinations of SSIPs can be identified from Fig. 2. The specific values of these four optimal parameter combinations, denoted as A, B, C, and D, are listed in Table 1. Here, $N = 0.3567$ represents the maximal entanglement of the system at $T = 0.8$ with $|\boldsymbol{J}| = 1$. In addition, the parameters corresponding to the maximal entanglement remain unchanged across different temperatures. Thus, maximal entanglement can be achieved by tuning the relative proportions of the SSIP components to the optimal combination.

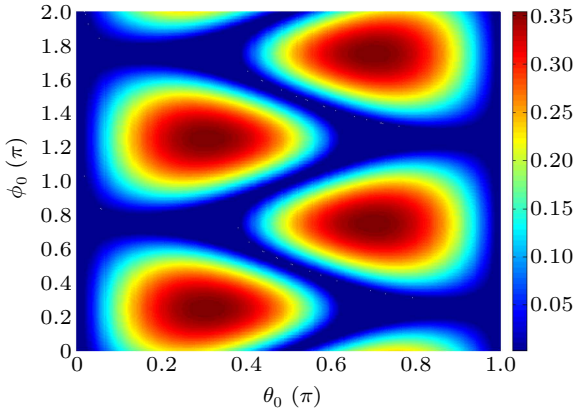


Fig. 2. Contour map of the negativity as a function of θ_0 and ϕ_0 for $T = 0.8$ and $|\boldsymbol{J}| = 1$.

Table 1. Four sets of optimal spin–spin coupling parameters.

	θ_0	ϕ_0	N
A	0.30367	0.25019	0.3567
B	0.69614	0.74962	0.3567
C	0.30367	1.25	0.3567
D	0.69614	1.7504	0.3567

3. Optimal combination of SOIPs

In this section, we consider the general anisotropic Heisenberg XYZ model with Dzyaloshinskii–Moriya (DM) interaction parameters. The Hamiltonian is given by

$$\begin{aligned} H' &= J_x\sigma_1^x\sigma_2^x + J_y\sigma_1^y\sigma_2^y + J_z\sigma_1^z\sigma_2^z + \boldsymbol{D}\cdot(\boldsymbol{\sigma}_1\times\boldsymbol{\sigma}_2) \\ &= J_x\sigma_1^x\sigma_2^x + J_y\sigma_1^y\sigma_2^y + J_z\sigma_1^z\sigma_2^z + D_x(\sigma_1^y\sigma_2^z - \sigma_1^z\sigma_2^y) \\ &\quad + D_y(\sigma_1^z\sigma_2^x - \sigma_1^x\sigma_2^z) + D_z(\sigma_1^x\sigma_2^y - \sigma_1^y\sigma_2^x), \end{aligned} \tag{3}$$

where J_i has the same form as in Section 2, $\boldsymbol{D}$ is the DM vector (arising from spin–orbit interaction),[35–38] and D_i denotes the i-axis component of $\boldsymbol{D}$. For simplicity, we set $|\boldsymbol{D}| = 1$ and express the components in spherical coordinates as

$$D_x = \sin\theta\cos\phi, \quad D_y = \sin\theta\sin\phi, \quad D_z = \cos\theta.$$

Using the same approach as in the previous section, we obtain the eigenstates and eigenvalues of H', calculate the eigenvalues of the partial transpose of the thermal state, and thus determine the negativity as a measure of thermal entanglement. (The detailed derivation is omitted here due to its complexity.) To analyze the dependence of thermal entanglement on θ and ϕ, we have generated numerous plots under a wide range of (θ_0, ϕ_0) values. From these results, we identify the optimal SOIPs corresponding to arbitrary SSIPs.

By systematically analyzing these figures, we find a general rule for determining the optimal SOIP: the optimal spin–orbit interaction vector is always parallel to the coordinate axis along which the SSIP has the largest component.

To illustrate this rule, Fig. 3 presents the evolution of thermal entanglement with DM parameters (θ, ϕ) in three representative cases. When J_x is the largest SSIP component, Fig. 3(a) shows that the entanglement reaches its maximum only when the DM vector is aligned with the x-axis (i.e., $\theta = 0.5\pi$, $\phi = 0$ or π). Similarly, when J_y is the largest component, Fig. 3(b) shows the maximum occurs when the DM vector aligns with the y-axis (i.e., $\theta = 0.5\pi$, $\phi = 0.5\pi$ or 1.5π). Finally, when J_z is dominant, Fig. 3(c) indicates the maximum entanglement arises when the DM vector aligns with the z-axis (i.e., $\theta = 0$ or π).

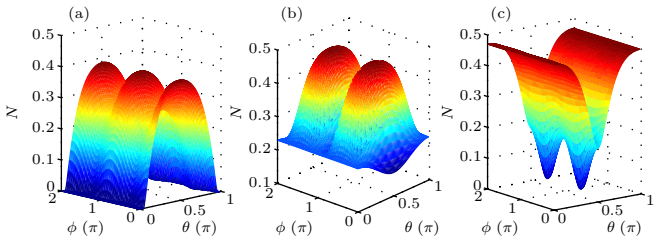


Fig. 3. Negativity plotted as a function of θ and ϕ for different SSIPs (θ_0 and ϕ_0) at $T = 0.8$: (a) $\theta_0 = 0.9\pi$, $\phi_0 = 0.1\pi$; (b) $\theta_0 = 0.5\pi$, $\phi_0 = 0.6\pi$; (c) $\theta_0 = 0.2\pi$, $\phi_0 = 1.5\pi$.

Furthermore, we plot Fig. 4 to provide a more detailed analysis of various SSIPs through regional division. In Fig. 4, the curve passing through point B corresponds to $J_x = J_z$, the curve through point D corresponds to $J_y = J_z$, and the straight line passing through points A and C corresponds to $J_x = J_y$. Using these boundaries, the diagram can be divided into three parts.

(a) In this region, J_x is the largest SSIP component, and the optimal spin–orbit interaction vector is parallel to the x-axis. This case includes two subregions: II ($J_x > J_z > J_y$) and III ($J_x > J_y > J_z$).

(b) In this region, J_y is the largest SSIP component, and the optimal spin–orbit interaction vector is parallel to the y-axis. This case includes two subregions: II′ ($J_y > J_z > J_x$) and III′ ($J_y > J_x > J_z$).

(c) In this region, J_z is the largest SSIP component, and the optimal spin–orbit interaction vector is parallel to the z-axis. This case includes two subregions: I ($J_z > J_x > J_y$) and I′ ($J_z > J_y > J_x$).

Thus, we can determine the optimal combination of SOIPs corresponding to any arbitrary set of SSIPs. In particular, to achieve higher entanglement, we focus on the optimal SOIP combinations associated with the four optimal SSIP combinations, denoted as points A, B, C, and D in Fig. 4 (corresponding to those in Table 1). At point A, where $J_x = J_y = J_z$, the system theoretically attains the same maximum entanglement for a DM vector in any direction. However, this scenario is difficult to realize in practice. Since point A lies at the intersection of the three regions, even a slight perturbation of the SSIP values can shift the system into a different region, thereby changing the corresponding optimal DM vector. By contrast, points B, C, and D lie in regions (b), (c), and (a), respectively. Consequently, for these three optimal SSIP combinations, the optimal spin–orbit interaction vectors are parallel to the y-, z-, and x-axes, respectively. Therefore, maximal entanglement can also be achieved by tuning the interaction parameters to align with these optimal directions.

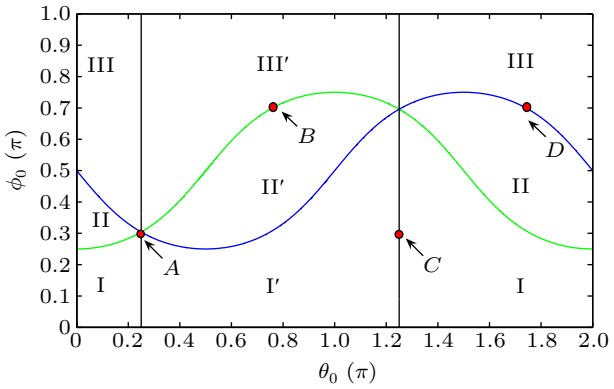


Fig. 4. Diagram showing the regions defined by SSIP components. The curve through point B corresponds to $J_x = J_z$, the curve through point D corresponds to $J_y = J_z$, and the straight line through points A and C corresponds to $J_x = J_y$.

4. Demonstration of adjusting parameters in an optical lattice

In this section, we apply the theoretical results obtained above to practical systems. In solid-state systems, spin–spin coupling arises from the Heisenberg exchange interaction, which is typically difficult to control. However, recent advances have proposed various methods for controlling spin–spin interactions. In ultracold atomic systems, adjustable spin interactions are usually realized by manipulating the wave function overlap between neighboring sites. In an optical lattice, the spin coupling can be tuned by varying external light or magnetic fields.[39–42]

We consider an atomic gas trapped in an optical lattice formed by two π-polarized laser beams counter-propagating along the y-axis, with frequencies below the atomic transition

frequency (i.e., a red-detuned lattice). An external static magnetic field $\boldsymbol{B}$ is applied along the z-axis, strong enough to polarize the ground-state spins along the quantization axis. The spinor system trapped in the lattice thus simulates a spin chain with an effective Hamiltonian[39,43]

$$H = -\sum_i \sum_{j\neq i} \left(J_{ij}^z S_i^z S_j^z + 2J_{ij}^x S_i^x S_j^x + 2J_{ij}^y S_i^y S_j^y \right), \tag{4}$$

with the coupling parameters

$$\begin{aligned} J_{ij}^x &= J_{ij}^{(\mathrm{opt})} - J_{ij}^{(\mathrm{mag})}/2, \quad J_{ij}^y = J_{ij}^{(\mathrm{opt})} - J_{ij}^{(\mathrm{mag})}/2, \\ J_{ij}^z &= J_{ij}^{(\mathrm{mag})}, \end{aligned} \tag{5}$$

where $J_{ij}^{(\mathrm{mag})}$ and $J_{ij}^{(\mathrm{opt})}$ denote the static magnetic dipole–dipole interaction and light-induced dipole–dipole interaction, respectively.

For simplicity, we consider a lattice consisting of only two sites, yielding

$$H = -2J_{12}^x S_1^x S_2^x - 2J_{12}^y S_1^y S_2^y - J_{12}^z S_1^z S_2^z. \tag{6}$$

This reduces to a two-qubit Heisenberg XYZ model corresponding to Eq. (1) with parameters $J_x = -2J_{12}^x = \sin\theta_0 \cos\phi_0$, $J_y = -2J_{12}^y = \sin\theta_0 \sin\phi_0$, and $J_z = -J_{12}^z = \cos\theta_0$. In this system, the angle ϕ_0 is restricted to 0.25π or 1.25π.[41]

As shown in our previous works,[40,41] both dipole–dipole interactions can be tuned by adjusting the transverse trapping widths and external laser parameters:

$$J_{12}^{(\mathrm{mag})} \propto 1/w_x, 1/w_z, \quad J_{12}^{(\mathrm{opt})} \propto 1/w_x, 1/w_z, U,$$

where w_x (w_z) is the trapping width along the x (z)-axis. There is no external trapping potential along the y-axis, except for the lattice potential. The laser intensity is defined as $U = \hbar|\Omega|^2/(6\Delta)$, where Ω is the Rabi frequency and Δ represents the laser detuning.

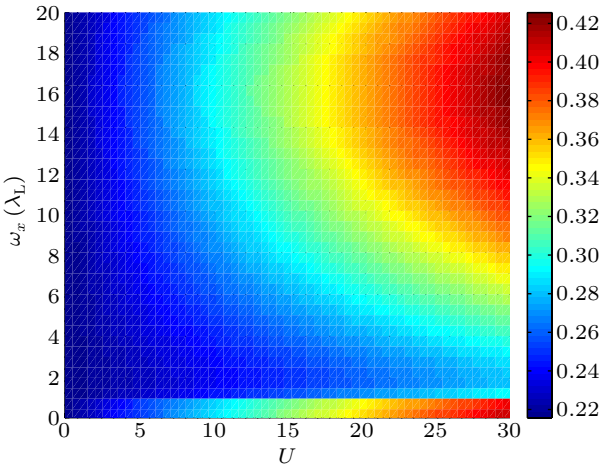


Fig. 5. Contour map of the angle θ_0 as a function of the trapping width and laser intensity, with $w_x = w_z$.

Figure 5 shows that the angle θ_0 can be tuned by adjusting the external optical fields. To achieve the optimal SSIP, we can realize $\theta_0 = 0.30367\pi$, which is close to the angles of points A and C in Table 1, by adjusting the transverse trapping potential and the intensity of the external laser. In fact, many parameters can be tuned, including the laser frequency and the magnetic field. The optical lattice system thus provides a versatile platform for demonstrating the optimization of the parameter combination.

5. Discussion and conclusion

In the previous section, we proposed a feasible scheme for adjusting SSIPs in an optical lattice. Furthermore, when DM interactions are present, the SSIPs can also be tuned to achieve the optimal parameter combination according to the direction of the DM vector. To control the DM vector direction, Ederer *et al.*[44] have proposed a scheme to invert the DM vector by modulating the electric field. In addition, Refs. [45–49] discuss various methods for adjusting the DM vector.

In summary, we have investigated the effects of interaction parameters on thermal entanglement in the general Heisenberg XYZ model. By analyzing the relation between parameter directions and entanglement, we identified the rule for the optimal spin–orbit interaction vector and obtained four optimal SSIP combinations and three effective SOIP combinations. Thus, the maximal entanglement of the system can be achieved by tuning the system parameters to these optimal combinations, which is feasible with current experimental technology.

Acknowledgments

This work was supported by the National Natural Science Foundation of China (Grant Nos. 11204061, 12204142, and 11904071), the Anhui Provincial Key Research and Development Project (Grant No. 2022b13020002), and the Outstanding Young Talents in College of Anhui Province (Grant No. gxyq2022059). We thank Prof. Wei-Ping Zhang for insightful discussions during the early stage of this work.

References

[1] Ekert A K 1991 *Phys. Rev. Lett.* **67** 661
[2] Bennett C H and Wiesner S J 1992 *Phys. Rev. Lett.* **69** 2881
[3] Neilsen M A and Chuang I L 2000 *Quantum computation and quantum information* (UK: Cambridge University Press) p. 4 (in Chinese)
[4] Horodecki R, Horodecki P, Horodecki M and Horodecki K 2009 *Rev. Mod. Phys* **81** 865
[5] Zou H Y and Wang W 2023 *Chin. Phys. Lett.* **40** 057501
[6] Qian X J and Qin M P 2023 *Chin. Phys. Lett.* **40** 057102
[7] Lin H Y, He R Q, Guo Y B and Lu Z Y 2024 *Chin. Phys. B* **33** 117504
[8] Kane B E 1998 *Nature* **393** 133
[9] Zad H A, Zoshki A, Ananikian N, Jascur M and Michal J 2022 *J. Magn. Magn. Mater.* **559** 169533
[10] Sørensen A and Klaus M 1999 *Phys. Rev. Lett.* **83** 2274

[11] Zhang D W, Chen J P, Shan C J, Wang Z D and Zhu S L 2013 *Phys. Rev. A* **88** 013612
[12] Natu S S, Pixley J H and Das Sarma S 2015 *Phys. Rev. A* **91** 043620
[13] Loss D and DiVincenzo D P 1998 *Phys. Rev. A* **57** 120
[14] Burkard G, Loss D and DiVincenzo D P 1999 *Phys. Rev. B* **59** 2070
[15] Bodoky F and Blaauboer M 2007 *Phys. Rev. A* **76** 052309
[16] Trauzettel B, Bulaev D V, Loss D and Burkard G 2007 *Nat. Phys.* **3** 192
[17] Mosshammer K and Brandes T 2014 *Phys. Rev. B* **90** 134305
[18] Van Diepen C J, Hsiao T K, Mukhopadhyay U, Reichl C, Wegscheider W and Vandersypen L M K 2021 *Phys. Rev. X* **11** 041025
[19] Senthil T, Marston J B and Fisher M P A 1999 *Phys. Rev. B* **60** 4245
[20] Nishiyama M, Inada Y and Zheng G Q 2007 *Phys. Rev. Lett.* **98** 047002
[21] Schecter M, Flensberg K, Christensen M H, Andersen B M and Paaske J 2016 *Phys. Rev. B* **93** 140503
[22] Wang D, Wiebe J, Zhong R, Gu G and Wiesendanger R 2021 *Phys. Rev. Lett.* **126** 076802
[23] Asoudeh M and Karimipour V 2005 *Phys. Rev. A* **71** 022308
[24] Zhang G F and Li S S 2005 *Phys. Rev. A* **72** 034302
[25] Kheirandish F, Akhtarshenas S J and Mohammadi H 2008 *Phys. Rev. A* **77** 042309
[26] Mohamed A A, Rahman A and Aldosari F M 2023 *Alex. Eng. J.* **66** 861
[27] Li Q H, Miao C Z and Xu Y L 2023 *J. Supercond. Nov. Magn.* **36** 957
[28] Amazioug M and Daoud M 2024 *Phys. Lett. A* **493** 129245
[29] Bouafia Z, Oumennana M, Mansour M and Ouchni F 2024 *Appl. Phys. B* **130** 94
[30] Li D C and Cao Z L 2008 *J. Phys.: Condens. Matter* **20** 325229
[31] Li D C and Cao Z L 2009 *Opt. Commun* **282** 1226
[32] Li D C, Li X M, Li H, Tao R, Yang M and Cao Z L 2015 *Chin. Phys. Lett.* **32** 050302
[33] Li D C, Wang X P, Li H, Li X M, Yang M and Cao Z L 2016 *Chin. Phys. Lett.* **33** 050301
[34] Vidal G and Werner R F 2002 *Phys. Rev. A* **65** 032314
[35] Dzyaloshinsky I 1958 *J. Phys. Chem. Solids* **4** 241
[36] Moriya T 1960 *Phys. Rev.* **117** 635
[37] Moriya T 1960 *Phys. Rev. Lett.* **4** 228
[38] Moriya T 1960 *Phys. Rev.* **120** 91
[39] Zhang W P, Pu H, Search C and Meystre P 2002 *Phys. Rev. Lett.* **88** 060401
[40] Zhao X D, Xie Z W and Zhang W P 2007 *Phys. Rev. B* **76** 214408
[41] Zhao X D, Zhao X, Jing H, Zhou L and Zhang W P 2013 *Phys. Rev. A* **87** 053627
[42] Gross K, Search C P, Pu H, Zhang W P and Meystre P 2002 *Phys. Rev. A* **66** 033603
[43] Pu H, Zhang W P and Meystre P 2001 *Phys. Rev. Lett.* **87** 140405
[44] Ederer C and Spaldin N A 2006 *Phys. Rev. B* **74** 020401
[45] Fujisawa M, Shiraki K, Okubo S, Ohta H, Yoshida M, Tanaka H and Sakai T 2009 *Phys. Rev. B* **80** 012408
[46] Rigol M and Singh R R P 2007 *Phys. Rev. B* **76** 184403
[47] Rigol M and Singh R R P 2007 *Phys. Rev. Lett.* **98** 207204
[48] Chutia S, Friesen M and Joynt R 2006 *Phys. Rev. B* **73** 241304
[49] Vedmedenko E Y, Udvardi L, Weinberger P and Wiesendanger R 2007 *Phys. Rev. B* **75** 104431